(12) INTERNATIONAL APPLICATION PUBLISHED UNDER THE PATENT COOPERATION TREATY (PCT)

(19) World Intellectual Property Organization
International Bureau

(43) International Publication Date
8 January 2009 (08.01.2009)

PCT

(10) International Publication Number
WO 2009/004665 A2

(51) International Patent Classification:
*C09K 19/02* (2006.01)

(21) International Application Number:
PCT/IT2008/000444

(22) International Filing Date: 30 June 2008 (30.06.2008)

(25) Filing Language: English

(26) Publication Language: English

(30) Priority Data:
CS2007 A000032 29 June 2007 (29.06.2007) IT

(71) Applicant *(for all designated States except US)*: **Universita della Calabria** [IT/IT]; Via P. Bucci 7-11 /B, loc Arcavacata, 87036 RENDE (CS) (IT).

(72) Inventors; and
(75) Inventors/Applicants *(for US only)*: **BARBERI RICCARDO** [IT/IT]; Via G. Verdi n°160/C, 87036 RENDE (CS) (IT). **BARTOLINO ROBERT** [IT/IT]; Via Salerno, 87036 RENDE (CS) (IT). **LOMBARDO GIUSEPP** [IT/IT]; Via G. Ungaretti n°59, 87036 RENDE (CS) (IT). **CIUCHI FEDERICA** [IT/IT]; Via C. Menotti n°64/B, 87036 RENDE (CS) (IT). **DE SANTO MARIA PENELOPE** [IT/IT]; Via G. Verdi n° 160/C, 87036 RENDE (CS) (IT). **VIRGA EPIFANIO GUIDO** [IT/IT]; Via XX Settembre 41, 27100 PAVIA (IT). **AYEB HABIB** [IT/IT]; Via A. Savinio, 87036 RENDE (CS) (IT). **DURAND GEORGES** [IT/IT]; 16, rue de Chateaufort, 91400 ORSAY (IT). **SONNET ANDRE' MATHIAS** [GB/GB]; 6A WINTON CIRCUS,, SALTCOASTS, SCOTLAND (GB).

(74) Agent: **PERROTTA ALDO**; Piazzetta T. Campanella 3, I - 88068 SOVERATO (CZ) (IT).

(81) Designated States *(unless otherwise indicated, for every kind of national protection available)*: AE, AG, AL, AM, AO, AT, AU, AZ, BA, BB, BG, BH, BR, BW, BY, BZ, CA, CH, CN, CO, CR, CU, CZ, DE, DK, DM, DO, DZ, EC, EE, EG, ES, FI, GB, GD, GE, GH, GM, GT, HN, HR, HU, ID, IL, IN, IS, JP, KE, KG, KM, KN, KP, KR, KZ, LA, LC, LK, LR, LS, LT, LU, LY, MA, MD, ME, MG, MK, MN, MW, MX, MY, MZ, NA, NG, NI, NO, NZ, OM, PG, PH, PL, PT, RO, RS, RU, SC, SD, SE, SG, SK, SL, SM, SV, SY, TJ, TM, TN, TR, TT, TZ, UA, UG, US, UZ, VC, VN, ZA, ZM, ZW.

(84) Designated States *(unless otherwise indicated, for every kind of regional protection available)*: ARIPO (BW, GH, GM, KE, LS, MW, MZ, NA, SD, SL, SZ, TZ, UG, ZM, ZW), Eurasian (AM, AZ, BY, KG, KZ, MD, RU, TJ, TM), European (AT, BE, BG, CH, CY, CZ, DE, DK, EE, ES, FI, FR, GB, GR, HR, HU, IE, IS, IT, LT, LU, LV, MC, MT, NL, NO, PL, PT, RO, SE, SI, SK, TR), OAPI (BF, BJ, CF, CG, CI, CM, GA, GN, GQ, GW, ML, MR, NE, SN, TD, TG).

**Published:**
— *without international search report and to be republished upon receipt of that report*

(54) **Title:** LIQUID CRYSTAL MIXTURE AND ITS USE FOR BISTABLE OR MULTISTABLE ELECTRO-OPTICAL DEVICES

(57) **Abstract:** Nematic liquid crystals, in particular conditions, assume locally and sometime only temporarily configurations characterized by a biassic order. This fact allows to connect between them uniaxial nematic textures with different topology without complete fusion of the nematic order, i.e. without the need to reduce the scalar order parameter to zero. The control of these transitions with electric fields allows to realize bistable or multistable displays of new conception. In fact two bistable or multistable textures are separated from a barrier of a well defined potential that it is determined from a biassic intermediate state, that connects said textures, determining the reorientation without rotation of the nematic director. Such mechanism is known in scientific literature as "order reconstruction". From now on in this document it will be indicated as "Biaxial Order Reconstruction in Nematics" or with acronym "BORN". The scope of the present invention is to realize mixtures of calamitic nematic liquid crystals with materials that favour the tendency to assume a biaxial order, in order to reduce the external electric field intensity necessary to reconstruct of the order.

WO 2009/004665 A2

# Liquid crystal mixture and its use for bistable or multistable electro-optical devices

## 1 Introduction

### 1.1 State of the art

All commercial nematic liquid crystal displays (NLCD) are based upon changes of optical properties of thin cells obtained by applying a suitable external electric field.
In general NLCD are made of two parallel glasses, few micron apart, (1 μm=$10^{-6}$m) confining the nematic material. The elongated molecules possess a dielectric anisotropy, hence are easily realigned along the external field.
The mean molecular alignment is described by a vector $\vec{n}$, the director, which represents the average orientation of molecules long axes. If no field is applied, the nematic assumes a stable configuration corresponding to the minimum of its elastic free energy.
The electric field drives then the liquid crystal into a high energy texture.
In all commercial display all textural changes appear overcoming a threshold called "Freedericksz transition" characteristic of a textural bulk bifurcation.
The nematic orientation at the surface is fixed and when the field is switched off the nematic relaxes visco-elastically back to the initial equilibrium configuration. The system is monostable, because it always relaxes towards the same energy state in absence of external excitation. In all commercial displays the anchoring at the surface is strong (ideally infinite) and the texture changes are monostable.
Bistability or multistability are essential for displays; it means that two or more states are stable in absence of applied field.
This property allows an infinite multiplexing of passive matrix displays. It suppresses the need of refreshing permanent pictures, it decreases the consumption for quasi-permanent pictures by allowing a refreshment rate comparable with the frame rate and it suppresses the blinking, due to the contrast decrease of relaxing textures in monostable devices.
Most of commercial NLCD use multistable pixels via monostable textural changes controlled by transistors or other electronic devices. This is the well known active matrix technology, TFT, where each pixel is associated with one individual Thin Film Transistor. Although well developed, this technology remains expensive since it is difficult to realize at least $10^6$ transistors without any defects on the surface of the display.

### 1.2 Bistable nematic display

It is possible to obtain NLCD with pixel having bistable or multisable texture without any additional electronic devices. An ideal bistable pixel should present two equilibrium states separated by an energy barrier. The barrier height should prevent the spontaneous transition among states, but it should allow to an external field to control the transitions.

1.2.1 Old bistable Technologies

Berreman and Heffner developed a cholesteric bistable cell [1]. They doped a nematic with a small quantity of cholesteric and filled a cell with strong oblique anchoring condition at the surfaces. The two bistable states are uniform tilted texture and $2\pi$ twisted texture. The cholesteric pitch is such that a spontaneous twist of $\pi$ is present in the cell, hence the uniform and $2\pi$ twisted textures have the same energy. The intermediate state corresponds to the nematic bulk director almost perpendicular to cell plates due to the strong alignment induced by the external electric field. The main drawback of this display is the difficulty to reproduce industrially uniform oblique anchoring with standard materials and to match the cholesteric pitch in a wide range of temperatures.
Furthermore the multiplexing is quite complex.
The Berreman-Heffner display belongs to the general case of switching of bistable textures with strong anchoring conditions at the surface. In this particular case the transition are among textures separated by a $2\pi n$ twist, n integer.
In order to allow $\pi$ twist changes, it would be necessary to rotate the director in one of the two confining surfaces. This change is topologically forbidden when the surfaces are fixed and possess strong anchoring conditions. It would be allowed in presence of weak anchoring , i.e. when the surface director is completely reoriented by the external field.
A simple example of this situation is the so-called planar anchoring where, in the absence of any field, molecules are parallel to the substrate in a well defined direction. Above a threshold, resulting from the symmetry of pure planar anchoring, it exists a surface anchoring bifurcation between the two equivalent $+\pi$ or $-\pi$ surface orientations. This well known bifurcation is called the "surface anchoring breaking". In this case the director alignment is perpendicular to the confining surface and can be obtained by electrodes on the anchoring plates and a nematic with positive dielectric anisotropy [2].
When the field is switched off slowly above the anchoring breaking threshold, the cell relaxes to the initial planar state, while when the field is switched off rapidly, a backflow mechanism come into play forcing the surface to the opposite orientation and inducing a $\pi$-twist on the bulk texture. The surface bifurcation can then control bulk texture changes which would be topologically impossible for fixed boundaries.
The problem of this technology is to realize reproducible weak anchoring in wide temperature range in order to obtain anchoring bifurcation at reasonable low fields.
Other bistable devices use special morphology of confining surfaces which gives rise to controlled defects creation and annihilation, the geometry used is usually a hybrid cell, i.e. a homeotropic plate and a planar one.
In reference we give a list of patents related to bistable switching of nematics and cholesterics [3,4,5,6,7].
All previous methods are based upon nematic textural changes, i.e. local reorientation of nematic director $\overline{n}$.
This is actually one of the component of the whole order parameter of the liquid crystal, which is a traceless tensor of rank 2. Formally it is written as $\overline{\overline{Q}} = \langle \overline{m}\overline{m} - \frac{\overline{\overline{I}}}{3} \rangle = S\left( \overline{nn} - \frac{\overline{\overline{I}}}{3} \right)$, where $\overline{m}$ is a unit vector along each molecule, the brackets <> means an ensemble average and $S$ is the scalar order parameter varying from -1/2 to 1. The system is non polar, $\overline{n}$ e $-\overline{n}$ are equivalent, but as soon as $\overline{n}$ direction is fixed in one surface, it is possible to follow the texture and define bend and twist of 0, $\pi$ o $2\pi$ travelling across the cell and ending to the other surface.

In all previous texture changes, either monostable or bistable, S is supposed to be constant and $\overline{n}$, the long axis of order tensor, changes slowly its direction $\overline{\overline{Q}}$.

1.2.2 Biaxial order reconstruction (BORN)

Another way to connect topologically distinct textures is to reorient locally the single molecule varying hence the average orientation, i.e. the long axis of $\overline{\overline{Q}}$, without rotation.
This method is known in literature as "order reconstruction" (Biaxial Order Reconstruction in Nematics – BORN).
The BORN can be achieved using a strong electric field. See for example Fig. 1a: $\overline{\overline{Q}}$ is locally directed along $\hat{x}$ and can be "reconstructed" along $\overline{E}$, axis $\hat{z}$ (Fig. 1b), without any director rotation but with a continuous deformation of the ellipsoid shape which is represented by $\overline{\overline{Q}}$, passing through from an horizontal elongated shape (Fig. 1a) to a vertical elongated one (Fig.1b). This deformation is obtained by electric coupling of molecules along the direction of the field and appears overcoming a threshold $|E_{th}|$. A simple calculation, equating the electric coherence length $\xi_E$ to the nematic-isotropic coherence length $\xi_{NI}$ [8,9,10], gives a high $|E_{th}|$, in the range 50-500 Volt/μm (V/μm) quite high for practical use.
The previous estimate of $|E_{th}|$ is pessimistic. The order reconstruction under applied field looks like the one which appears across a core of a defect like ½ disclination line [8]. Here the order reconstruction is imposed by topological constraints which forces $\overline{n}$ in one direction on one side of the core and in the perpendicular one in the other. The brutal solution proposed earlier implies a nematic fusion with $S$=0. A biaxial solution at lower energy has been proposed in [11]. Since the biaxial coherence length $\xi_B$ is slightly larger than $\xi_{NI}$ we expect the threshold field in the range 10/50 V/μm, still too large for practical purposes. The aim of this patent is to find a way to reduce $\xi_B$, hence $|E_{th}|$.
The nematic order reconstruction cannot be explained by a simple description at S constant, like Freedericksz transition. The Landau-de Gennes description is required with the order tensor formalism $\overline{\overline{Q}}$. $\overline{\overline{Q}}$ eigenvectors give the preferred molecular orientation and their eigenvalues $\lambda_1$, $\lambda_2$, $\lambda_3$, the corresponding degree of order in that direction. When the material is in the isotropic phase, all eigenvalues are zero, no preferred orientation exists. If the nematic has a uniaxial calamitic state, one privileged axis exists and its eigenvalue (for example $\lambda_1$) is maximum and defines the phase order parameter. If a nematic has a biaxial phase all eigenvalues are different.
Usually the nematic equilibrium state is isotropic or uniaxial, depending on the temperature. Biaxial domains have been forecast and observed near defects or in nanoconfined systems.
There are also discotic nematic (intrinsically biaxial) [12,13] which possess a stable biaxial phase but we will not discuss this subject in details.

The free nematic energy density, using Landau-De Gennes formalism, is: $F_b = F_t + F_d + F_e + F_s$ where $F_t$ is the thermotropic energy density and describes the phase diagram of the system : isotropic phase, uniaxial, biaxial. Usually this energy is expanded in Taylor series around $\overline{\overline{Q}}=0$ until the fourth order: $F_t = a \cdot tr\left(\overline{\overline{Q}}^2\right) + \frac{2b}{3} tr\left(\overline{\overline{Q}}^3\right) + \frac{c}{2}\left(tr\left(\overline{\overline{Q}}^2\right)\right)^2$, only $a$ is temperature dependent $a=\alpha$ (T-$T_C$) and $\alpha>0$. When $T<T_C$ only the nematic phase is stable.
The $b$ coefficient is temperature independent and is a measure of biaxial tendency of the system: small b values favour biaxial ordered states.
For uniaxial states, the thermotropic energy minimum gives the following value of order parameter: $S_{eq} = \frac{1}{4c}\left(-b + \sqrt{b^2 - 24ac}\right)$. Varying $a$, $b$ or $c$, the range of temperature in which each phase is stable varies: raising temperature nematic phase appears and then the isotropic one.
$F_d$ is the elastic energy density and well describe the energy cost of spatial variation of $\overline{\overline{Q}}$.
Let use for simplicity one elastic constant approximation $L$: $F_d = \frac{L}{2} \cdot (\nabla \overline{\overline{Q}})^2$ with L>0.
When an electric field is applied, an electric energy density $F_e$ has to be taken into account as well,
$F_e = -\frac{\varepsilon_0}{2} \overline{E} \cdot \varepsilon \overline{E}$, where $\varepsilon_0$ is the vacuum dielectric permeability and $\varepsilon$ the dielectric tensor that describes the anisotropic response of liquid crystal to the applied field.
$F_s$ is the surface energy due to the interaction between liquid crystal and surfaces. In our case we suppose the interaction strong, i.e. infinite anchoring energy.
The equilibrium state of the system is given by the minimum of free energy density with the imposed constraints at the boundaries. A system of non linear coupled differential equations, derived from Eulero Langrange ones, has to be solved:

$$\sum_{j=1}^{3} \frac{\partial}{\partial x_j}\left(\frac{\partial F_b}{\partial q_{i,j}}\right) = \frac{\partial F_b}{\partial q_i} \quad (1) \text{ where } i = 1..5, \text{ and } q_{i,j} = \frac{\partial q_i}{\partial x_j},$$

where $\overline{\overline{Q}}$ is symmetric traceless tensor and it was expressed in terms of $\overline{\overline{Q}} = \begin{pmatrix} q_1 & q_2 & q_3 \\ q_2 & q_4 & q_5 \\ q_3 & q_5 & -q_1 - q_4 \end{pmatrix}$.
Solving (1) keeping fixed the electric potential $\Delta V$, the order tensor $\overline{\overline{Q}}$ is known in each point of the cells. The field distribution inside the cell is determined solving simultaneously the static Maxwell equations.
We want to determine the threshold behaviour of our system when the $b$ coefficient varies, i.e. when the liquid crystal tends to assume biaxial configurations. The coherence biaxial length of pure liquid crystal is given by: $\xi_B = \sqrt{\frac{L}{bS_{eq}}}$; $L$ is around $10^{-12}$ N, $S_{eq}$=0.6 and $b$=1.6·$10^6$ N/m$^2$ (values comparable to the ones of 5CB used in our experiments), hence $\xi_B$ is of the order of few nanometers.

To obtain the order reconstruction is necessary that the electric coherence length equates the biaxial coherence length: $\xi_E \approx \xi_B$. If $b$ decreases, keeping constant the scalar order parameter, $\xi_B$ increases and the threshold decreases.

Fig. 4 shows the threshold variation as a function of $b$ at constant $S_{eq}$ calculated by numerical method based upon Landau De Gennes model. It is evident that $|E_{th}|$ can be reduced to a few Volt/micron, values that are compatible with the applications and electronic drivers used to multiplex the NLCD.

# 2 Invention

## 2.1 Experimental results

We doped nematic liquid crystal with suitable molecules demonstrating the possibility of controlling the order reconstruction by an electric field. We checked experimentally that low percentages of biaxial molecules or molecules assuming biaxial arrangements added to nematic liquid crystal with high $\Delta\varepsilon$ can reduce sensibly the BORN threshold on timescale larger than 1 μsec. This result shows that it is possible to reduce BORN threshold in a time interval suitable for practical devices, using doped nematic materials. A further threshold decrease has been observed for times above 1 msec. This could be explained supposing that the molecules concentration during the transition adjusts itself, by diffusion, reducing further the BORN threshold.
These local changes require time of the order of msec. It is possible then to choose opportunely the guest concentration depending on the device response time.
Biaxial or discotic dopant concentrates around nematic defect lines, hence their presence favours BORN

## 2.2 Materials

We prepared mixtures of standard nematics at high $\Delta\varepsilon>0$ and low volume percentages of molecules allowing BORN at few V/μm, in a wide range of temperatures. Locally the nematic behaviour is similar to the cholesteric one. The dopants chosen are:

- molecular materials with negative or weak dielectric anisotropy;
    - Materials made of biaxial molecules. We consider biaxial molecules with a ratio between the two principal molecular axes length and width less than 4 and greater or equal to 1, the third molecular axis is shorter than the two principal axis;
- Discotics materials, i.e. molecular materials which presents discotic phases.
- Oligomers with low molecular weight. In order to be soluble in nematics, these materials should be made of monomers with high polarizability without intrinsic nematic phase or nematics linked to a main chain (main chain polymers).
- Stabilized nanostructures with possibly a large electrical or magnetic biaxial susceptibility.

## 2.3 The new proposed technology

Using the field induced order reconstruction BORN and suitable materials, we have demonstrated that we can induce transitions between two bistable textures topologically non-equivalent at low enough electric field. We use the standard high dielectric anisotropy and low viscosity materials, nematic or cholesteric, but with conveniently chosen low concentrations dopants. The biaxial order reconstruction is a bulk transition and it occurs in presence of strong anchoring (ideally infinite) at confining boundaries.
No adjustment of material properties to the cell geometry is required (i.e. cholesteric pitch related to cell thickness) to guarantee bistability. Depending on the geometry, we can build

new kind of writing or erasing systems with addressing time below 1 μs or we can induce transitions between two stable states 0-twist and π-twist, in planar cells.
This transition among textures non topological equivalent is similar to the one observed in anchoring breaking devices without need of special treatments on anchoring surfaces with low anchoring energy. It is also possibile to control creation/annihilation of nematic defects. Since discotic or biaxial dopants concentrate around defects the presence favours the BORN.

# 3 Bulk order reconstruction experiments

## 3.1 Standard experiment and sample preparation

To demonstrate the order parameter reconstruction effect, we have chosen first as a specific example a simple geometry with a pure well known compound (5CB, 4-cyano-4'-n-pentyl biphenyl). Then we will describe subsequent experiments with doped samples to show how this effect can be implemented in practice for devices at low threshold and weak temperature dependence.

To demonstrate the order parameter reconstruction and measure its threshold, we chose the symmetric geometry is shown in Fig.2a. The two plates are transparent conductive electrodes allowing the application of an electric field $\overline{E}$ in $\hat{z}$ direction. They are supposed to have infinite anchoring energy and low pretilt angle $\vartheta_S$. The cell thickness is $d$. Fig.2a shows a slightly splayed texture. Fig.2b shows a quasi $\pi$-bend texture. They are topologically non equivalent: it is not possible deforming elastically and continuously one into the other. The only way to go from splay to bend texture, with infinite boundaries conditions, is to reconstruct in the bulk the director from $\hat{x}$ direction to $\hat{z}$ direction with a total variation of 90°. This is well known to happen locally if one places a ±1/2 disclination in the centre of the cell. In absence of defects, we want to study a fast and homogeneous order reconstruction which allows the transition from splay Fig.2a to bend Fig.2b. If the splay texture of Fig.2a is symmetric with respect to the centre of the cell, the transition starts in the middle where $\overline{E}$ and $\overline{n}$ are mutually perpendicular. When the field is switched off, in practice, the $\pi$-bend texture relaxes into the $\pi$-twist since the twist deformation is energetically favourite. The two deformations are topologically equivalent.

If the starting splayed texture is non symmetric, the transition moves nearest the surface with the lower pretilt but the mechanism is always the same: initial splay, bend, when the field is on, and finally twist when the field is switched off. The order reconstruction can be so near to the surface to be practically indistinguishable from anchoring breaking, but is observed even in strong anchoring conditions.

The transition is observed by a polarized light microscope. Naturally in the case of the initial symmetric splay texture, just before the reconstruction, in presence of the electric field, the director $\overline{n}$ is aligned almost along the field except for symmetry in a $\pi$-splayed thin wall in the centre, whose thickness is comparable to the electric coherence length, which connects $\overline{n}$ from $\hat{z}$ to $\hat{x}$ and back to $\hat{z}$ (Fig.3a). This wall is strongly biaxial. Away from the wall the nematic is uniaxial with a scalar order parameter higher than the initial one due to the aligning force of the electric field. When the field overcomes the threshold $E_{th}=V_{th}/d$ ($V_{th}$ applied d.d.p $d$ cell thickness), BORN is observed: the biaxial wall is destroyed and a uniform uniaxial orientation appears in the centre of the cell (Fig.3b).

We chose as nematic material 5CB uniaxial below 35.2°C with a high dielectric anisotropy $\Delta\varepsilon = 15$ at T=26°C. 5CB is a good model system since most of its material properties are well known and can be used in the numerical calculations increasing the accuracy.

The cell is made of two conductive ITO glass plates. The strong oblique symmetrical anchorings are produced by unidirectional rubbing of a polymer LQ1800 (from Hitachi), previously spin coated and oven dried, following a standard procedure [14]. A thick film gives strong anchoring. For this reason we used for the spin coating procedure a 20% in

weight solution of LQ1800 in 1-methyl-2-pyrolidinone. Lower concentrations give thinner, less homogeneous films and lower anchoring energy.
The two unidirectional rubbings are assembled parallel to obtain the right geometry of Fig.2a. The pretilt has been measured with an independent optical method [15] and for this materials $\vartheta_S = (10 \pm 1)°$, with a strong anchoring energy. Calibrated spherical spacers (1÷4 μm) fix the cell thickness. The birefringence measured at room temperature is typical of a quasi planar texture, as expected.

### 3.2 Typical observations

The cell is connected to a pulse generator which can vary independently pulse amplitude V and width τ. The pulse is sent manually to the cell.
Textural changes are checked using a polarized microscope at a controlled angle with respect to the surface alignment direction.
We describe the behaviour of a 2μm cell. The temperature is kept at 32°. The pulse width is 1 msec and we slowly increase the voltage. Up to 15 V we observe only a transient optical effect: after the pulse the distorted texture relaxes back to the initial splay with a relaxation time of about 4 msec. At V=15.5 Volt bright spots appear. Increasing again at $V_{th}$=16.0 Volt, the entire pixel is now covered by a uniform bright texture independent of surface irregularities and of microsphere position. After the pulse, the texture relaxes back to the initial state by means of slow motion of disclination lines, originating from the pixel border and from the microspheres that move parallel to the confining plates.
We send now electrical pulses of the same amplitude at a low rate of 1 every 5 seconds to reproduce regularly the new texture to analyze. Rotating the analyzer alone of 35°, the new texture appears black, the initial planar texture is now bright. Rotating the sample the black results independent of the rotation angle whereas the outside planar texture presents the classical periodic dark and bright aspect. This indicates that the new created texture presents rotatory power. This is typical of a twisted texture. These optical properties are in fact the same of a π-twisted cell obtained by breaking a weak planar anchoring on SiO [2,16]. We know from independent measurements that the used LQ1800 (20% in weight in 1-methyl-2-pyrolidinone) induces on 5CB a strong anchoring which cannot be broken at 32°C by electric field up to 50V/μm, maximum amplitude applied to the cell without burning it. As we used a much lower field $V_{th}$=8.0 V/μm, we cannot have broken the surface anchoring. The uniform onset of the new texture shows that is a bulk effect and the splay-bend wall is in the centre of the cell (Fig.3). The onset of the new texture above $V_{th}$ can be interpreted as field order reconstruction of the nematic director from the initial planar texture towards the vertical field orientation. Under field, there should exist a transient π-bend texture corresponding to Fig.2b. As soon as the field is switched off, since the twist constant is two times lower than the bend one, the bend texture decays towards a π-twist shown in Fig.2c.
We measured the threshold in the cell thickness range allowed by our present technology (from 1 to 4 μm) and we verified that the $V_{th}$ is proportional to the cell thickness *d*, as expected for the order reconstruction. Below 1μm, the thickness is not well defined due to microsphere size dispersion.
In principle it is possible working with thicknesses higher than 4 μm.

### 3.3 Order reconstruction dynamics

We studied the threshold $E_{th}=V_{th}/d$ dependence on pulse width. The temperature is kept fixed at 32°C. A typical plot of $E_{th}$ vs $\tau$ is shown in Fig.5. In the range $0.1<\tau<3$msec, $E_{th}$ is practically independent of $\tau$. This seems to correspond to a static threshold. For shorter $\tau$ a sharp increase of $E_{th}$ is observed, which corresponds to a "dynamical" threshold. $E_{th}$ increases to force a fast evolution of the order reconstruction.
We present in Fig.6 the dependence of $E_{th}$ on T, when $\tau$ is fixed: $\tau$=0.1msec, 1msec e 10 msec. The threshold decreases and tends to zero approaching $T_C$.
In ref. 17, the authors showed that the wall onset and order reconstruction induced by an electric field are fast phenomena which end in times of the order of $\tau_{th}=(80 \pm 20)$ μs at room temperature.
We observed similar behaviours using a nematic mixture E7 from Merck with a dielectric anisotropy comparable to 5CB and optical and visco-elastic properties similar in a wider range of temperature $-20°<T<62.5°$C (Figs. 10,11,12).

## 4 Experiments with doped nematic in symmetric configuration

### 4.1 Materials properties

An industrializable nematic or cholesteric material must obviously present a low biaxial reconstruction threshold but it must obey practical constraints. In the discussed geometry of Fig. 2, it should present:

- a high positive dielectric anisotropy $\Delta\varepsilon$ to build the thin biaxial wall;
- a low enough viscosity, to reconstruct the wall rapidly;
- a wide nematic temperature range around room temperature for the nematic phase;
- good optical properties (transparency, birefringence, contrast, etc.)

Certainly it is possible to achieve the synthesis of new material nematic or cholesteric materials with large biaxiality, but in practice it is at present convenient to keep using the common calamitic nematic doped with compounds enhancing the biaxial tendency of the mixture, showing large decrease of the order reconstruction threshold from the pure nematic. Contrary to what one thought in the past, it was shown that one can obtain a complete miscibility between calamitic (rod-like) and biaxial (disc-like) molecules [18].
As a thermotropic calamitic nematic material is generally composed of elongated molecules with axial ratio in the order of 4 [8] (the axial ratio is defined as the length of the molecule divided by the diameter), in the next we are going to call biaxial all molecules with axial ratio less than 4 and greater than 1. Discotic molecules, i.e. molecular material which presents discotic phases, are a particular case of biaxial molecules. In first mixtures we doped the 5CB with different compounds with low concentrations. Of course as soon as we mix the 5CB with any dopants, we observe a change in $T_C$, proportional to the dopant concentration. If the dopant has no nematic phase or a nematic phase at lower $T_C$, the $T_C$ of the mixture is down shifted. If it has higher $T_C$ nematic phase, we observe an up shift. In practice we will take advantage of this property to increase or to decrease the temperature range of the mixture as a function of the desired reduced threshold. The $T_C$ shift gives an up or down shift of the threshold, which is not related to the intrinsic biaxiality, since the reconstruction depends only

on the relative temperature $T_C$-T. We then present our temperature dependent data versus the reduced temperature $T_C$-T.
All experiments, in order to be compared between with each other, are made using the cell geometry presented in Fig.2, with the same anchoring conditions, using LQ1800 as aligning films as described above for the experiment with pure 5CB.

### 4.2 5CB + MBBA

A well known molecule which is expected to align well in 5CB is MBBA, which presents a nematic phase at room temperature. $\Delta\varepsilon_{MBBA}$=-0.5, so that a 5CB and 2% MBBA mixture has a mean dielectric constant $\Delta\varepsilon$=14.6, 3% smaller than pure 5CB.
In the absence of electric field the nematic phase is uniaxial. The enhancement of the biaxiality of the mixture inside the thin $\pi$-splayed wall before the BORN is in first approximation due to the fact that the 5CB molecules tend to be aligned along the electric field and the MBBA molecules tend to be aligned perpendicular to the electric field. In this case the nematic order is strongly decreases (without vanishing) due to the strong applied frustration. The negative $\Delta\varepsilon_{MBBA}$ should increase the MBBA concentration in the $\pi$-splayed wall, independently from the biaxiality.
The reduction of the dielectric anisotropy of the mixture with respect to the pure 5CB should increase the $E_{th}$, but the comparison with the pure 5CB shows a reduction of $E_{th}$, as shown in Fig. 6 for $\tau$=0.1msec, $\tau$=1msec e $\tau$=10msec and for the temperature range $0<T_C-T<15C°$. The decrease of $E_{th}$, is due to the fact that this mixture tends to assume biaxial configurations easier than the pure 5CB.
The $E_{th}$ threshold decreases in average about 5%. This means that, if we use the values presented in the paragraph 1.2.2, the parameter $b$ varies from $1.610^6$ N/m$^2$ to $1.010^6$ N/m$^2$.

### 4.3 5CB + $BaTiO_3$

It is also possible to increase $E_{th}$ if the dopant increases $b$. This is the case of $BaTiO_3$, an anisotropic nanostructure, as shown in Fig. 7. The $BaTiO_3$ is a ferroelectric nano-particle (the particle size is lower than 50 nm) with a spontaneous polarization of 26 $\mu$C/cm$^2$ at room temperature, which tends to stabilize the calamitic nematic order of the 5CB. It is enough to add the 0.5% in weight to the 5CB to increase the $E_{th}$ . Also in this case we show the behaviour of $E_{th}$ for pulse lengths of $\tau$=1 msec or $\tau$=0.1 msec and for the temperature range $0<T_C-T<15C°$.

### 4.4 5CB + RM257

Now we use as dopant a diacrylate monomer RM257 from Merck. The monomer RM257 has negative dielectric anisotropy $\Delta\varepsilon \approx -2$ and presents a stable nematic phase in the range of temperature 70-126°C. This dopant was dissolved in the 5CB in the proportion of 2% .
For this mixture we measured $E_{th}$ for $\tau$ = 1msec and $\tau$ = 0.1msec for the temperature range $0<T_C-T<15C°$.
Observing the Fig. 8, we note a decreasing of $E_{th}$ comparable with the previous case of MMBA.

### 4.5 5CB + RM257 and conformational biaxiality

It is important to notice that, if we polymerize the monomer RM257, to obtain oligomer chains of typical length 2-100*nm*, we can increase further the biaxial susceptibility. If the oligomer chains are dissolved in the isotropic phase, statistically disordered, they tend to bend but do not form a cross-linked network as they are not long enough. Such short chain keeps a cylindrical symmetry around the orientation of the central monomer. These chains, relatively short, can be even dissolved in a uniaxial nematic phase. If the nematic becomes biaxial, the chain becomes also biaxial by increasing its curvature. This is a "conformational" biaxiality due to the variation of oligomers shape.
The oligomer has also another important property: by mixing a usual large molecular mass polymer with a nematic one, the order parameter usually decreases due to the entropy effect of the rigid oligomer chains. At large concentration, the large molecular mass polymer induces the isotropic melting of the nematic.
Such biaxial phase is easily reoriented by an electric field, with a low order reconstruction threshold. We expect then the oligomer effect to be much stronger than the one of the rigid molecule of the monomer.
The previous mixture of 98% of 5CB and 2% of RM257 was exposed to UV for wavelength in the range 359-400*nm* for 30s before filling the symmetric cell of Fig.2a. As shown in Fig.8 $E_{th}$ is reduced further compared to the previous case. Comparing the case of 5CB+monomer with the case of 5CB+oligomer (monomer exposed to UV), we notice that the reduction of $E_{th}$ depends on the UV exposure time. The optimum UV exposure time should correspond to the building of oligomers of good length to optimize the biaxial order reconstruction.
With our experiments we achieved a reduction of $E_{th}$ of about 10%. This means that this mixture reduces the value of $b$ from $1.610^6$ N/m$^2$ to $0.710^6$ N/m$^2$.

### 4.6 E7 + biaxial molecules

In the following we doped the commercial nematic E7, brand Merck, with molecules having strong biaxial or discotic conformation. The pure E7 has dielectric anisotropy comparable to 5CB and similar optical and visco-elastic properties in a larger temperature range -20 <T<62.5°C.
The first dopant that we have used, is a molecule having an H shape, ($C_{84}H_{98}O_{12}N_4Pt_2Cl_2$), where its graphical structure is represented in Fig.9. It is metallo-organic complex of palatine which is discotic with high molecular biaxiality.
The fig.10 illustrates the comparison of the threshold transitions $E_{th}$, between the pure E7 and the mixture of E7+H-shape for $\tau$=1msec, $\tau$=0.1msec and $\tau$=10msec for temperature range $0<T_C-T<40$ °C.
It is interesting to note that a strong decrease of the threshold $E_{th}$ for $\tau$ =10 msec, which is in the order of about 30%. This involves a strong decrease of the parameter $b$ from $1.6\text{x}10^6$ N/m$^2$ to almost $0.2\text{x}10^6$ N/m$^2$.
We have also investigated other mixture of E7 doped with biaxial metallo-organic molecules, as the PtAcAc ($C_{53}H_{56}O_8N_2Pt$), which is nematic between 185-250°C and the palladium complex AZPAC ($C_{29}H_{40}O_5N_2Pd$), which presents also nematic phase for the temperature range 94°C-102°C.
Also in these cases the dopant was added in low percentage (lower than 5%) showing the same positive effect but less effective than the H-shape molecule. We note that the AZPAC

has a small negative dielectric anisotropy, which reduces the dielectric anisotropy of the mixture with respect to the pure E7, while this parameter is unknown for the PtAcAc.
We have also seen a decrease of $E_{th}$ proportional to the concentration of the dopant, for small concentration of itself.

### 4.7 E7+Sartomer 349 and conformational biaxiality

We now use as dopant for the E7 a photo-polymerizable acrylate, Sartomer 349 (ethoxylated bisphenol A diacrylate) by Cray Valley, which does not present any mesophase. We prepared four mixtures with different concentrations $c$=1%, 2%, 3% and 4%. As it is expected, the Nematic-Isotropic $T_{N-I}$ temperature transition is down shifted by increasing the concentration $c$. The N-I transition temperatures are shown on table 1. We have measured for these mixtures $E_{th}$ as a function of $\tau$ at different temperature. Comparing with pure E7, for small $\tau$, we observe again a decrease of $E_{th}$, practically proportional to $c$. Fig.11 shows $E_{th}$ versus $T_C$-T for pure E7 and all the four mixtures at $\tau$=1msec. The gain, roughly proportional to $c$, is 6.1% for $c$=1%, 12.1% for $c$=2%, 19.0 for $c$=3%, 23.0% for $c$=4%, at $T_C$-T=18°C.
Fig.12 shows further decrease of $E_{th}$ of the mixture with respect to pure E7, after the mixture was exposed to UV to make oligomers similar to those already described in paragraph 4.5. In this case also we observe the effect of the conformational biaxialty due to the oligomers. Similar results are obtained even for other concentrations $c$ achieved if the mixtures are exposed to the UV.

## 5 Conclusion

We have proved the existence of nematic materials which can achieve biaxial order reconstruction for electric fields weak enough to be compatible with the standard techniques used in liquid crystal display technology. The main proposed application concerns the possibility for a nematic or a cholesteric to switch from an initial texture to a final topologically different one in order to induce an intrinsic bistability or multistability in the display pixels.

The biaxial nematic material must possess a large biaxial coherence length $\xi_B$ (small values of $b$ which depends on the third order term in the Landau-de-Gennes potential) at the room temperature, moreover viscosity and optical properties suitable for NLCD. As pure materials with these characteristics do not exist, we have shown that low concentration mixtures of a typical nematic material having large positive dielectric anisotropy ($\Delta\varepsilon>0$) with suitable biaxial molecules meet these requests and induce order reconstruction transitions with low electric threshold.

The best material we have found for these mixtures is an optimized oligomer of relatively small molecular mass. Obviously we can improve the reported threshold values by optimizing the dopant materials. Molecules which are strongly biaxial like "H-shape" molecules have provided good results.

It is important to note that it is possible to obtain low and temperature independent thresholds by dissolving in the nematic almost any kind of molecules with biaxiality different from the one of the host nematic.

Another effect, that was experimentally checked, concerns the fact that doping is more effective for long $\tau$ than for short $\tau$. For example, in Fig.10, $E_{th}$ decreases of about 30% for $\tau$=10msec and only 10% for $\tau$=1msec. It is therefore clear that this effect depends on phenomena like diffusion of dopant molecules in the nematic or cholesteric matrix. During the biaxial transition, the concentration of biaxial molecules can automatically arrange itself to induce the order reconstruction with lower electric field threshold. The variation of the concentration requires time, typically in the range of milliseconds and one can then choose the appropriate concentration of the dopant also depending on the response time required by the bistable device.

The order reconstruction is present not only in the geometry we used for our experiments (Fig.2) but also in presence of other phenomena like, for example, the creation and destruction of defects. The nematic defects (as well as cholesteric ones) present in fact biaxial states in the core [11]. It is important to note that all bistable devices proposed in references 4, 5, 6 and 7 change the nematic texture by means of the creation and destruction of defects. The mixtures proposed in this work can cause a remarkable decrease of the electric field threshold for all bistable displays reported in references and they are not restricted to the experiments described in this patent. The discotic/biaxial dopants tend also to concentrate around the calamitic nematic defects, because the nematic phase order is reduced in the core of a defect, hence favouring the BORN. In conclusion, the proposed mixtures are good materials for all bistable LCD technologies where bistable or multistabile textures are connected to each other by transient phenomena as bi-dimensional biaxial walls or monodimensional defects.

**Bibliography**

[1] D.W. Berreman, W.R. Heffner, *Bistable Liquid Crystal Twist Cell*, US 4239345.
[2] I. Dozov, M. Nobili, G. Durand, *Appl. Phys. Lett.*, vol **70**, 1179 (1997)
[3] G. Durand, R. Barberi, M. Giocondo, Ph. Martinot-Lagarde, *Bistable Liquid Crystal Display Device*, WO 9717632, EP 0859970
[4] R. Barberi, G. Durand, R. Bartolino, M. Giocondo, I. Dozov, J. Li, *Bistable Display Device Based on Nematic Liquid Crystal Allowing Grey Tones*, EP 0773468, US 5995173, JP 9274205
[5] G.P. Bryan-Brown, C.V. Brown and J.C. Jones, *Zenithal Bistable Nematic Display*, GB 95521106.6
[6] D. Sikharulidze, *Bistable Nematic Liquid Crystal Display Device*, GB2394781, US2003210375(A1), JP2004163867
[7] C.S. Kitson, A.D. Geisow, *Bistable Liquid Crystal Device*, EP1139151(A1), US6903790(B2), US2001028427(A1), JP2001296563
[8] P.G. de Gennes, J. Prost, The *Physics of Liquid Crystals*, Oxford Science Publications, Claredon Press, Oxford (1993)
[9] I. Lelidis, *Transitions de phases induites par un champ electrique dans les cristaux liquides*, PhD thesis, Universite de Paris Sud, Orsay, France (1994)
[10] P.R. Martinot-Lagarde, I. N. Dozov, *Bistable Liquid Crystal Display Device,* FR2814847(A1) *WO 02/27393 PCT/FR01/02996.*
[11] N. Schopohl, T.J. Sluckin, *Phys. Rev. Lett.*, vol **59**, 2582 (1987)
[12] L. J. Yu and A. Saupe, *Phys. Rev. Lett.*, vol **45**, 1000(1980)
[13] Sandeep Kumar, Sanjay Kumar Varshney, Angew. Chem., vol **112**, n.17, 3270 (2000)
[14] D.S. Seo, h. Matsuda, T. Ohide, S. Kobayashi, *Mol. Cryst. Liq. Cryst.*, vol **224**, 13 (1993)
[15] H.A. Van Sprang, *Mol. Cryst. Liq. Cryst.,* vol. **199**, 19 (1991)
[16] M. Monkade, M. Boix, G. Durand, *Europhys. Lett.*, vol. **5**, 697 (1988)
[17] R. Barberi, F. Ciuchi, G. Lombardo, R. Bartolino, and G. E. Durand, *Phys. Rev. Lett,* vol. **93**, 137801 (2004).
[18] D. Apreutesei, G. H. Mehl, *Chem. Commun.*, 2006, 609-611.

**Figure Captions**

Fig.1 Graphical representation of the nematic order tensor $\overline{\overline{Q}}$. a) the long axis of $\overline{\overline{Q}}$ locally along $\hat{x}$. b) the long axis of $\overline{\overline{Q}}$ is reconstructed along the electric field $\overline{E}$, in the $\hat{z}$ direction.

Fig.2 Cell geometry involved in our experiments: a) splay texture, b) π-bend texture, c) π-twist texture;

Fig.3 a) π-splay wall in the centre of the cell, before the BORN; b) homeotropic texture in the middle of the cell after the BORN.

Fig.4 Electric field threshold $E_{th} = V_{th}/d$ as a function of the coefficient $b$, calculated using the order tensor representation as described in1.2.2.

Fig.5 Electric field threshold $E_{th}=V_{th}/d$ for pure 5CB at 32°C as a function of the pulse width τ.

Fig.6 Electric field threshold $E_{th}=V_{th}/d$ for pure 5CB and for the mixture 5CB + 2% MBBA, for three τ values (0.1msec, 1 msec, 10msec) as a function of temperature $0<T_C-T<15$ °C.

Fig.7 Electric field threshold $E_{th}=V_{th}/d$ for pure 5CB and for the mixture 5CB + 0.5% $BaTiO_3$, for three τ values (0.1msec, 1 msec, 10msec) as a function of temperature $0<T_C-T<15$ °C.

Fig.8 Electric field threshold $E_{th}=V_{th}/d$ for pure 5CB and for the mixture 5CB + 2% RM257, for two τ values (0.1msec, 1 msec) as a function of temperature $0<T_C-T<15$ °C, before and after UV curing.

Fig.9 Graphical representation of the "H-shape" molecule.

Fig.10 Electric field threshold $E_{th}=V_{th}/d$ for pure E7 and for the mixture E7 + 3% H-shape molecules, for three τ values (0.1msec, 1 msec, 10msec) as a function of temperature $0<T_C-T<40$ °C.

Fig.11 Electric field threshold $E_{th}=V_{th}/d$ for pure E7 and for the mixture E7 + Sartomer 349, at the concentrations $c$=1%, 2%, 3% and 4%, for τ=1 msec as a function of temperature $0<T_C-T<40$ °C.

Fig.12 Electric field threshold $E_{th}=V_{th}/d$ for pure E7 and for the mixture E7 + 3% Sartomer 349, for τ=1 msec as a function of temperature $0<T_C-T<40$ °C before and after UV curing.

**Figure Captions**

Fig.1 Graphical representation of the nematic order tensor $\overline{\overline{Q}}$. a) the long axis of $\overline{\overline{Q}}$ locally along $\hat{x}$. b) the long axis of $\overline{\overline{Q}}$ is reconstructed along the electric field $\overline{E}$, in the $\hat{z}$ direction.

Fig.2 Cell geometry involved in our experiments: a) splay texture, b) $\pi$-bend texture, c) $\pi$-twist texture;

Fig.3 a) $\pi$-splay wall in the centre of the cell, before the BORN; b) homeotropic texture in the middle of the cell after the BORN.

Fig.4 Electric field threshold $E_{th} = V_{th}/d$ as a function of the coefficient $b$, calculated using the order tensor representation as described in1.2.2.

Fig.5 Electric field threshold $E_{th}=V_{th}/d$ for pure 5CB at 32°C as a function of the pulse width $\tau$.

Fig.6 Electric field threshold $E_{th}=V_{th}/d$ for pure 5CB and for the mixture 5CB + 2% MBBA, for three $\tau$ values (0.1msec, 1 msec, 10msec) as a function of temperature $0<T_C-T<15$ °C.

Fig.7 Electric field threshold $E_{th}=V_{th}/d$ for pure 5CB and for the mixture 5CB + 0.5% $BaTiO_3$, for three $\tau$ values (0.1msec, 1 msec, 10msec) as a function of temperature $0<T_C-T<15$ °C.

Fig.8 Electric field threshold $E_{th}=V_{th}/d$ for pure 5CB and for the mixture 5CB + 2% RM257, for two $\tau$ values (0.1msec, 1 msec) as a function of temperature $0<T_C-T<15$ °C, before and after UV curing.

Fig.9 Graphical representation of the "H-shape" molecule.

Fig.10 Electric field threshold $E_{th}=V_{th}/d$ for pure E7 and for the mixture E7 + 3% H-shape molecules, for three $\tau$ values (0.1msec, 1 msec, 10msec) as a function of temperature $0<T_C-T<40$ °C.

Fig.11 Electric field threshold $E_{th}=V_{th}/d$ for pure E7 and for the mixture E7 + Sartomer 349, at the concentrations $c$=1%, 2%, 3% and 4%, for $\tau$=1 msec as a function of temperature $0<T_C-T<40$ °C.

Fig.12 Electric field threshold $E_{th}=V_{th}/d$ for pure E7 and for the mixture E7 + 3% Sartomer 349, for $\tau$=1 msec as a function of temperature $0<T_C-T<40$ °C before and after UV curing.

## Claims

1. Nematic or cholesteric liquid crystal mixture for bistable or multistable electro-optical devices governed by order reconstruction effect like BORN to decrease the BORN electric threshold, where BORN is used to switch the device at least between two liquid crystal textures which are locally stable and said textures are connected by means of creation/destruction of a bidimensional biaxial wall or monodimensional defects, even in presence of strong boundary anchoring conditions, characterized by a nematic with high dielectric anisotropy $\Delta\varepsilon>5$ or a cholesteric liquid crystal with high dielectric anisotropy $\Delta\varepsilon>5$ or a mixture of nematic + cholesteric with high dielectric anisotropy $\Delta\varepsilon>5$, to vary the cholesteric pitch, and at least one of the materials listed in the following in any possible percentage:
    a. calamitic rod like molecular materials with weak dielectric anisotropy $\Delta\varepsilon$ ($0\leq\Delta\varepsilon\leq5$) or negative dielectric anisotropy;
    b. materials composed by biaxial molecules, whose axial ratio between the two principal molecular axis, i.e. between the length and the width of the molecule, is less than 4 and greater or equal than 1, the third molecular axis being shorter than the two other principal axis;
    c. molecular materials which present discotic order;
    d. oligomers with low molecular weight and composed by a number of monomers between 2 and 100;
    e. nanostructures with large dielectric or magnetic biaxial susceptibility.
2. Use of a mixture according to claim 1 in an electro-optical device characterized by bistability or multistability;
3. Use of a mixture in a bistable electro-optical device according to claim 2 characterized by the fact that works with two textures, one uniform planar or weakly twisted in which molecules tend to be parallel to each other, and the other which differs for a twist of about $\pm180°$ with respect to the first one, where the switching is controlled by bulk order reconstruction like BORN.
4. Use of a mixture in a bistable electro-optical device according to claim 3 characterized by the fact the BORN is localized close to a boundary surface to orient the liquid crystal mixture along the vertical electric field, starting from a planar or quasi-planar orientation, replacing, even in presence of strong anchoring, by means of the BORN bulk effect, the mechanism of anchoring breaking, which requires a weak anchoring.
5. Use of a mixture in a bistable electro-optical device according to claims 2 or 3 or 4, characterized by the fact that the BORN is used to create or destroy defects.

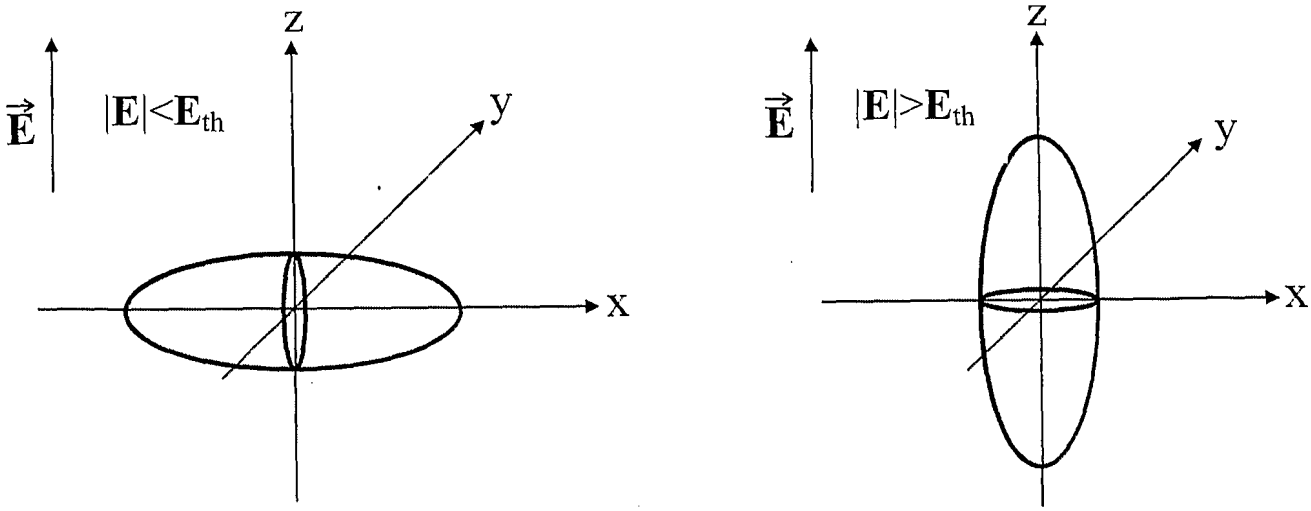


Initial Configuration
(a)

Order Reconstruction
along ***E***
(b)

FIG. 1

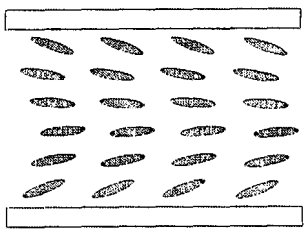

splay

FIG. 2a

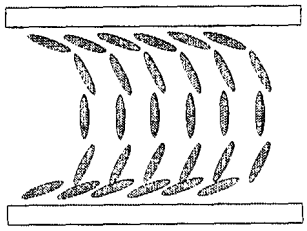

π-bend

FIG. 2b

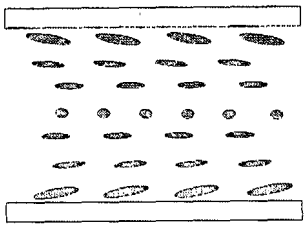

π-twist

FIG. 2c

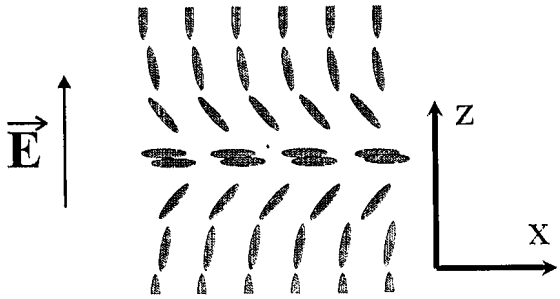


Before BORN

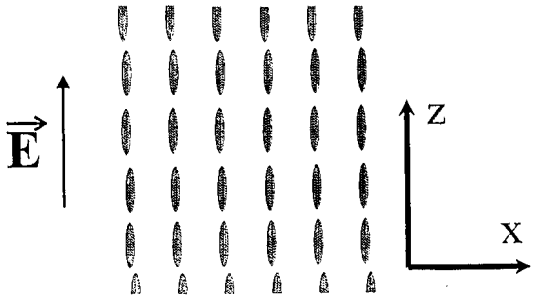


After BORN

FIG. 3a

FIG. 3b

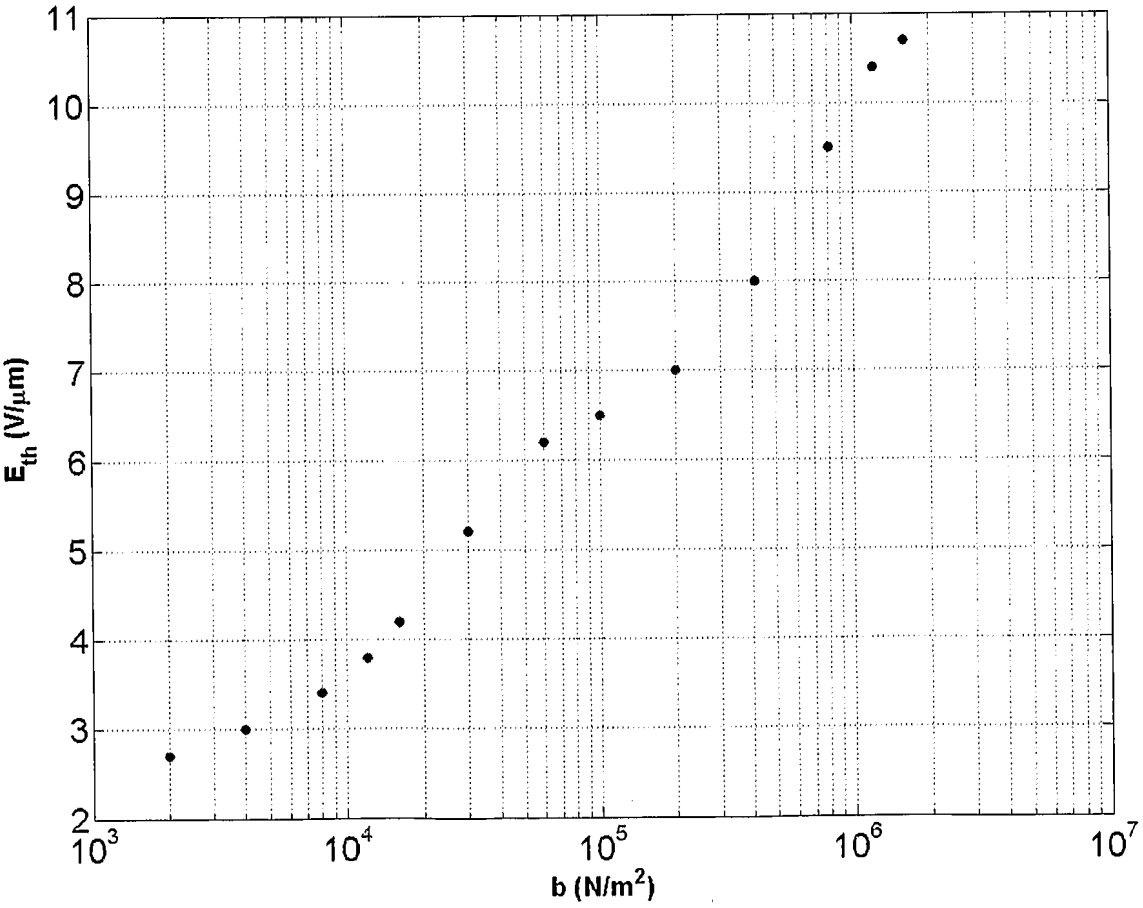


FIG. 4

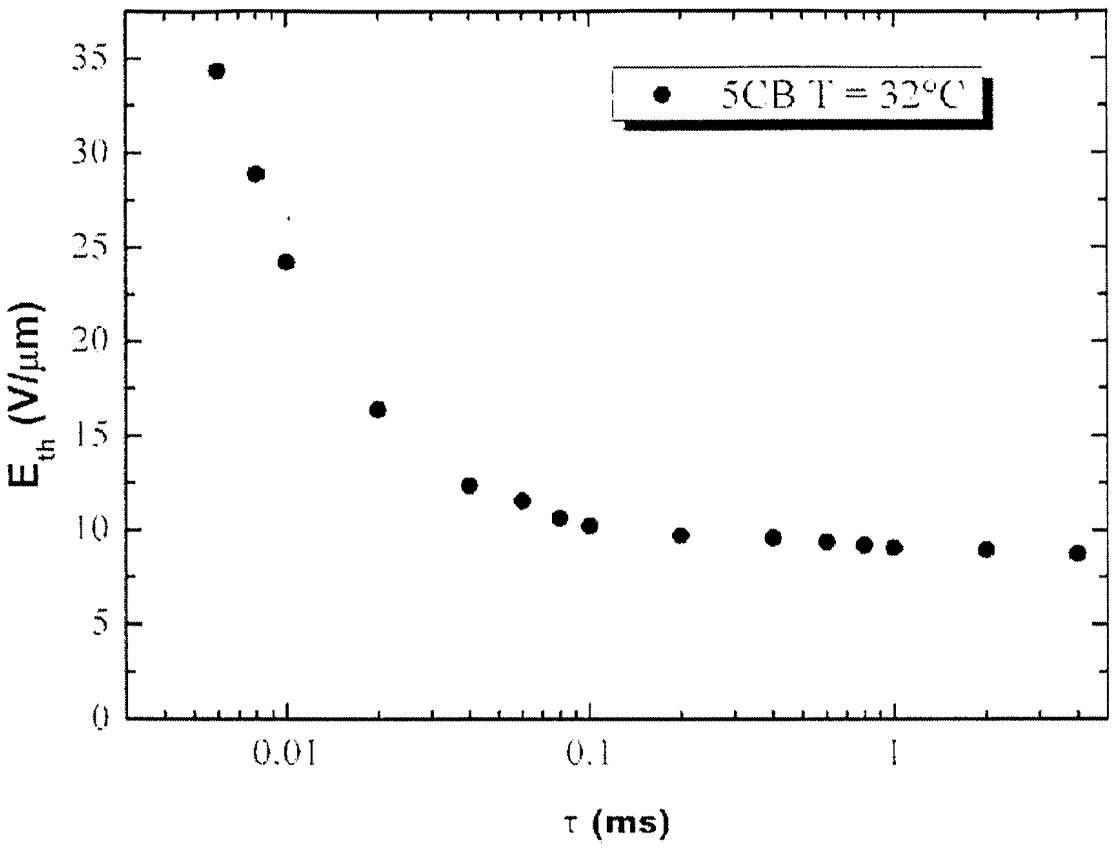
5CB T = 32°C
$E_{th}$ (V/μm)
τ (ms)
0
5
10
15
20
25
30
35
0.01
0.1
1

FIG. 5

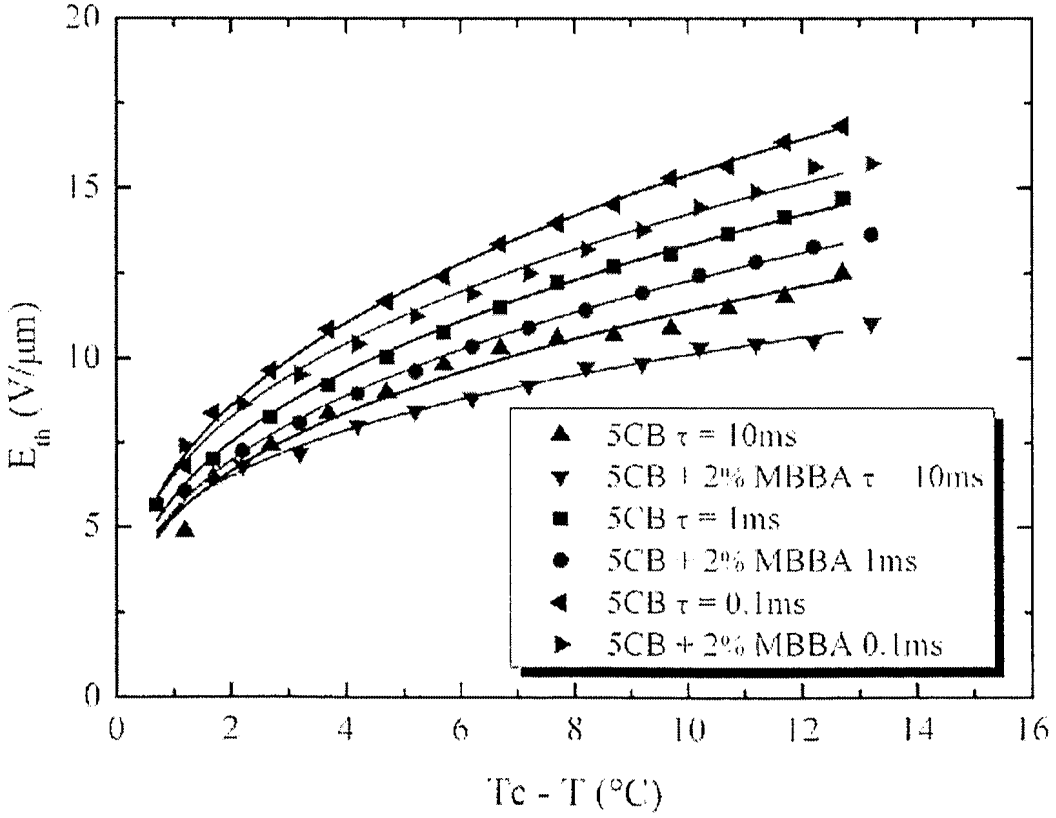
5CB τ = 10ms
5CB + 2% MBBA τ 10ms
5CB τ = 1ms
5CB + 2% MBBA 1ms
5CB τ = 0.1ms
5CB + 2% MBBA 0.1ms
$E_{th}$ (V/μm)
Tc - T (°C)
0
5
10
15
20
0
2
4
6
8
10
12
14
16

FIG. 6

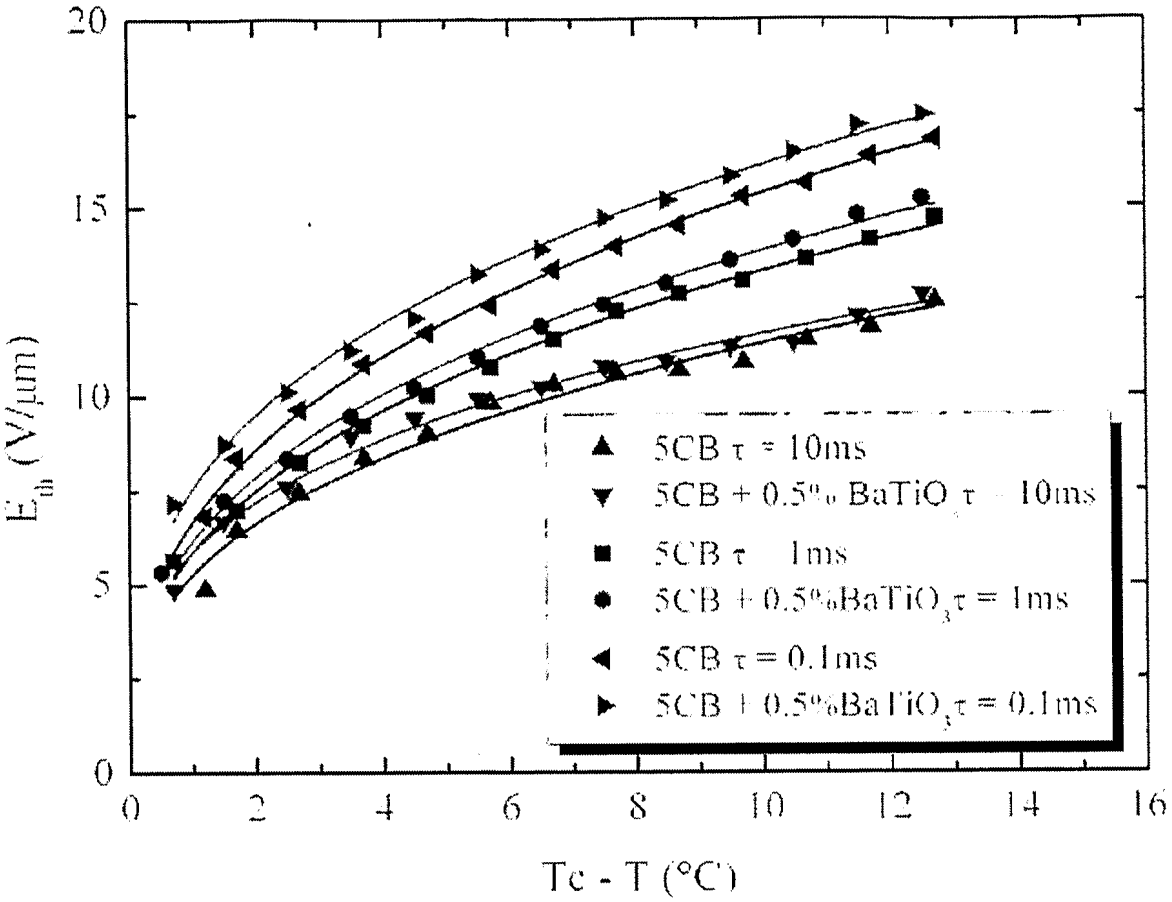
20
15
10
5
0
0
2
4
6
8
10
12
14
16
$E_{th}$ (V/μm)
Tc - T (°C)
5CB τ = 10ms
5CB + 0.5% BaTiO$_3$ τ = 10ms
5CB τ = 1ms
5CB + 0.5%BaTiO$_3$ τ = 1ms
5CB τ = 0.1ms
5CB + 0.5%BaTiO$_3$ τ = 0.1ms

FIG. 7

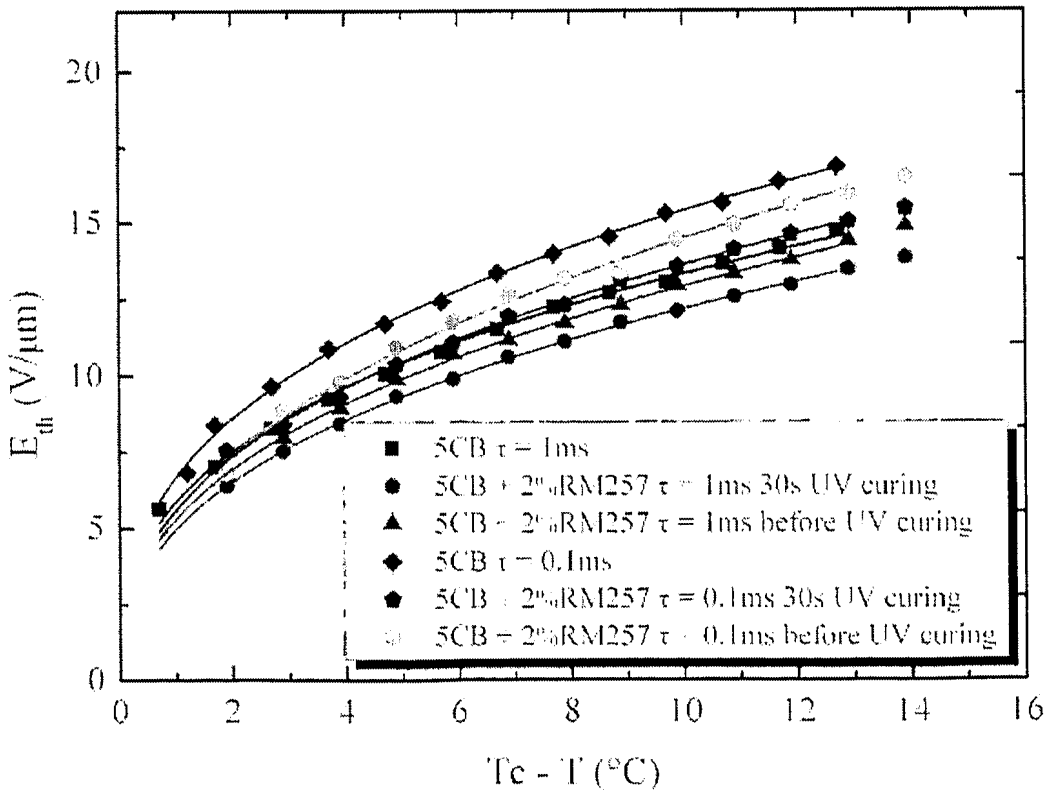
20
15
10
5
0
0
2
4
6
8
10
12
14
16
$E_{th}$ (V/μm)
Tc - T (°C)
5CB τ = 1ms
5CB + 2%RM257 τ = 1ms 30s UV curing
5CB + 2%RM257 τ = 1ms before UV curing
5CB τ = 0.1ms
5CB + 2%RM257 τ = 0.1ms 30s UV curing
5CB + 2%RM257 τ = 0.1ms before UV curing

FIG. 8

H-shape molecule

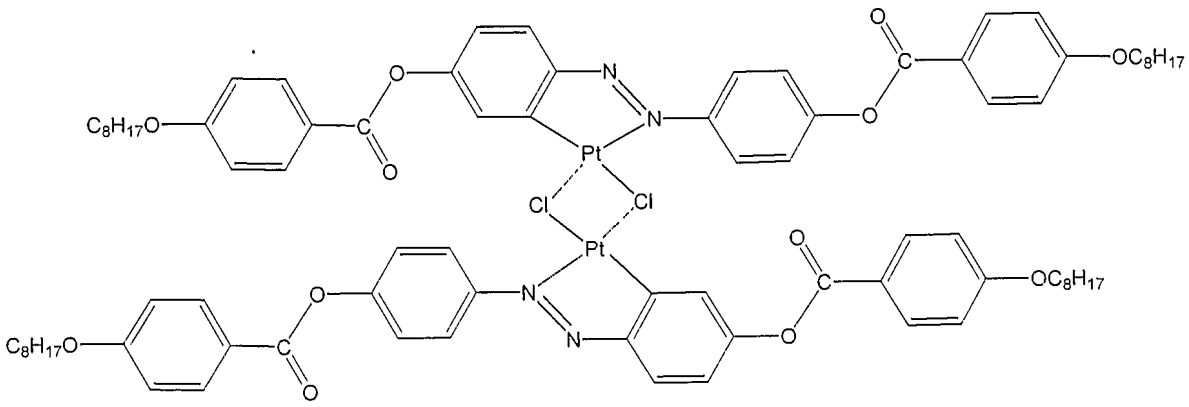


FIG. 9

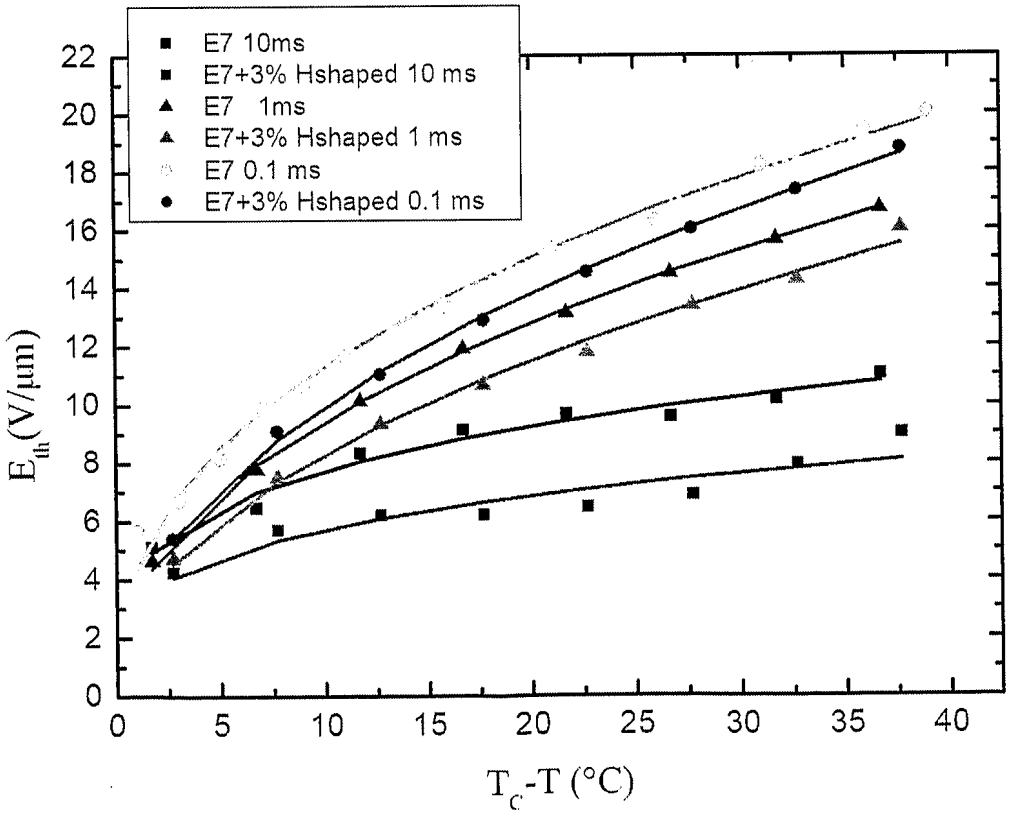


FIG. 10

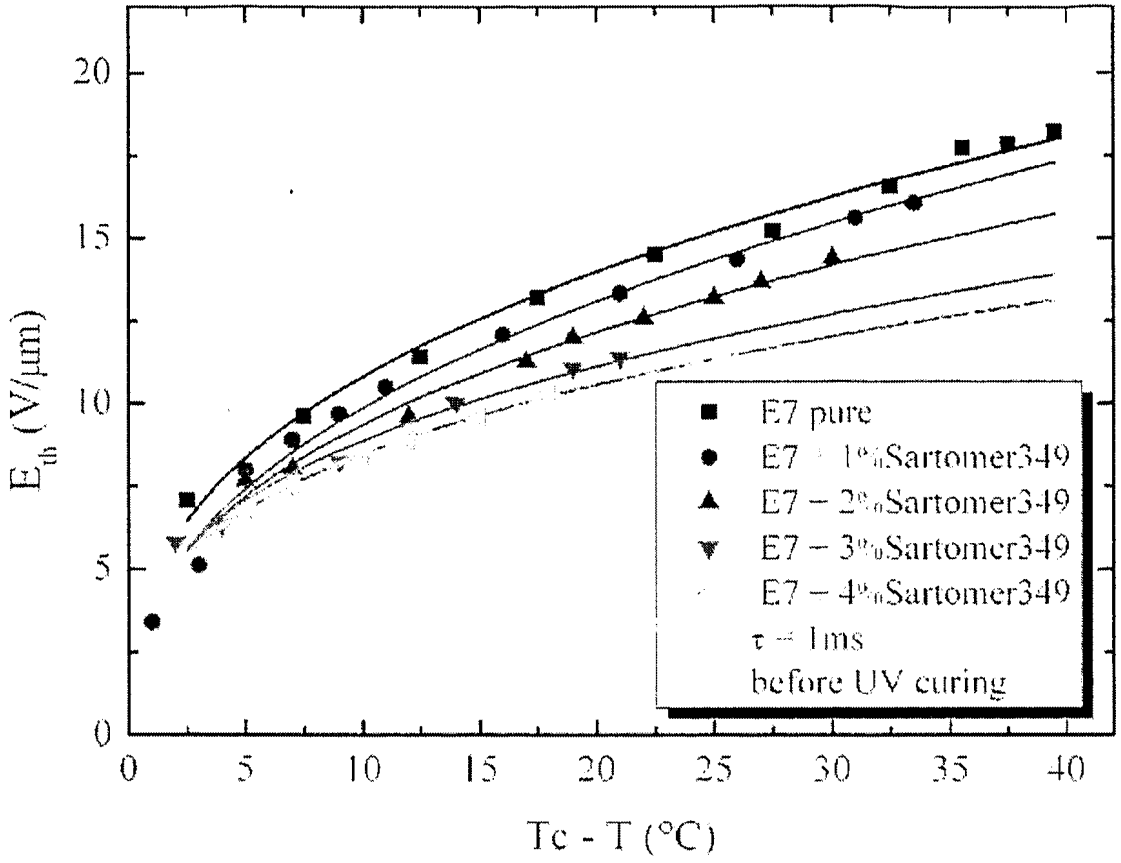
E7 pure
E7 + 1%Sartomer349
E7 + 2%Sartomer349
E7 + 3%Sartomer349
E7 + 4%Sartomer349
τ = 1ms
before UV curing
$E_{th}$ (V/μm)
Tc - T (°C)

FIG. 11

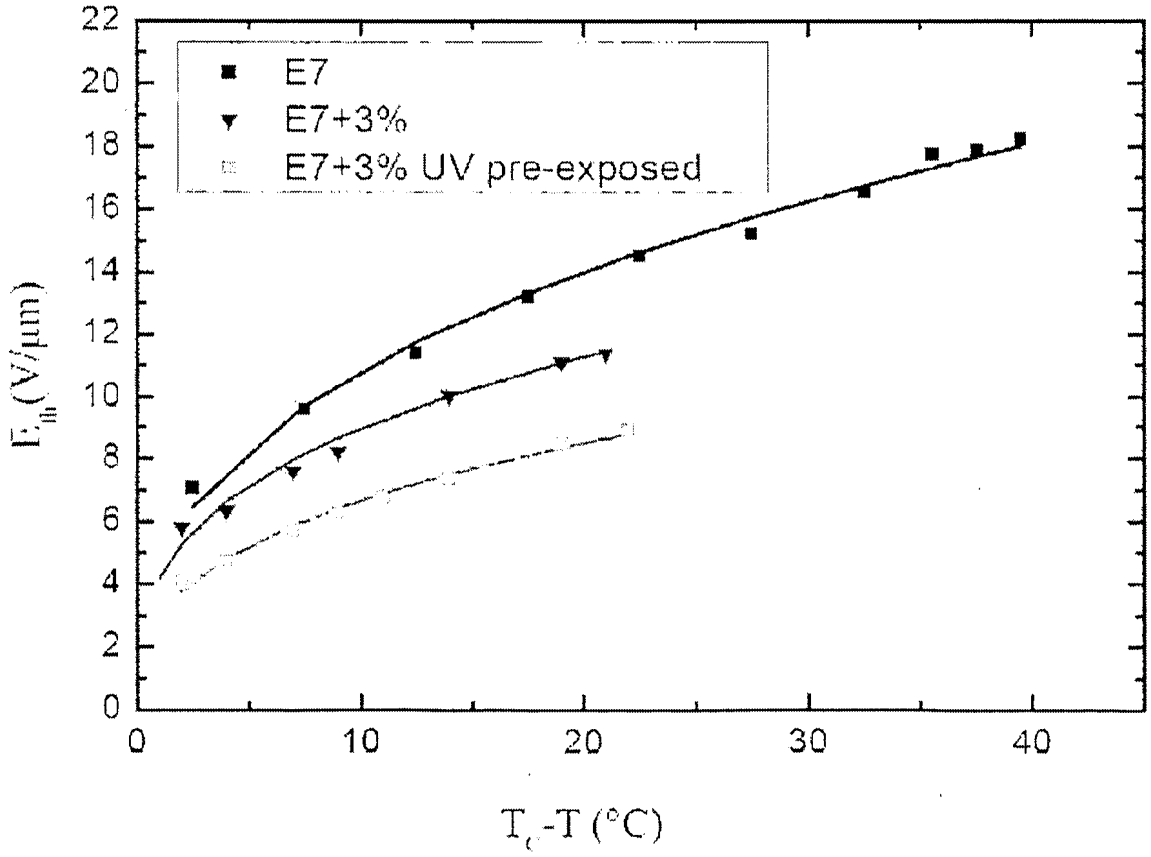
E7
E7+3%
E7+3% UV pre-exposed
$E_{th}$ (V/μm)
$T_c$-T (°C)

FIG. 12

| Concentration of Sartomer 349 in E7 | N-I transition (°C) |
|---|---|
| 1% | 57 |
| 2% | 52 |
| 3% | 45 |
| 4% | 40 |

Table 1